Mechanics of Materials 158 (2021) 103886

Contents lists available at ScienceDirect

Mechanics of Materials

journal homepage: www.elsevier.com/locate/mechmat

Mechanical reliability analysis of nanoencapsulated phase change materials combining Monte Carlo technique and the finite element method

Josep Forner-Escrig [a], Rosa Mondragón [a,*], Leonor Hernández [a], Roberto Palma [b]

[a] Department of Mechanical Engineering and Construction, Universitat Jaume I, Av. de Vicent Sos Baynat, s/n, 12071, Castelló de la Plana, Spain
[b] Department of Structural Mechanics and Hydraulic Engineering, University of Granada, Campus Universitario Fuentenueva, Edf. Politécnico, 18071, Granada, Spain

ARTICLE INFO

Keywords:
Monte Carlo
Finite element method
Nanoencapsulated phase change materials
Mechanical reliability
Sensitivity analysis

ABSTRACT

Nanoencapsulated phase change materials (nePCMs) are one of the technologies currently under research for energy storage purposes. These nePCMs are composed of a phase change core surrounded by a shell which confines the core material when this one is in liquid phase. One of the problems experimentally encountered when applying thermal cycles to the nePCMs is that their shell fails mechanically and the thermal stresses arising may be one of the causes of this failure. In order to evaluate the impact of the uncertainties of material and geometrical parameters available for nePCMs, the present work presents a probabilistic numerical tool, which combines Monte Carlo techniques and a finite element thermomechanical model with phase change, to study two key magnitudes of nePCMs for energy storage applications of tin and aluminium nePCMs: the maximum Rankine's equivalent stress and the energy density capability. Then, both uncertainty and sensitivity analyses are performed to determine the physical parameters that have the most significant influence on the maximum Rankine's stress, which are found to be the melting temperature and the thermal expansion of the core. Finally, both a deterministic and a probabilistic failure criterion are considered to analyse its influence on the number of predicted failures, specially when dispersion on tensile strength measurements exists as well. Only 1.87% of tin nePCMs are expected to fail mechanically while aluminium ones are not likely to resist.

1. Introduction

The world demand of energy is estimated to increase by 26% and CO_2 associated emissions will continue rising by 10% by the year 2040 with respect to those registered in 2017 (International Energy Agen, 2019). In order to reduce the environmental problems, efforts are made by several scientific communities to foster the use of renewable energies, which exploit natural resources –unlimited on a human timescale– without generating polluting emissions. The present work focuses exclusively on solar energy and more precisely, on its application to concentrated solar plants (CSP), since solar energy is the renewable energy presenting the major potential for exploitation of energy (International Energy Agen, 2011). Nevertheless, one of the main cons of solar energy is its intermittence since energy production depends largely on weather/climate conditions. Consequently, owing to the high demand of energy in the electricity market, gaps between generation and supply of energy cannot be tolerated to guarantee the correct operation of the electrical grid. One of the characteristics that makes CSP stand out among other renewable energy technologies is the possibility of incorporating Thermal Energy Storage (TES) systems to mitigate the previously mentioned generation gaps. TES systems appear to be a field of research on its own nowadays for energetic transition towards renewable energies within the context of green policies (Gil et al., 2010; Xu et al., 2015; Akhmetov et al., 2016; Mondragón et al., 2017).

The focus of the present work lays on one of the technologies under research for TES systems in concentrated solar plants: nanofluids (Choi and Eastman, 1995), which is the name received by the colloidal suspension of nanoparticles (less than 100 nm) in a base fluid to enhance its thermal properties. One of the advantages of these suspensions is that, due to the Brownian motion of the particles within the base fluid, nanofluids combine the good thermal properties of nanosolids with the transport properties of the fluid avoiding clogging or settling problems.

The thermal energy storage capability of the nanofluids is a key parameter of their performance for TES purposes. Although the enhancement of sensible heat storage capability of commonly used nanoparticles (metal oxides or carbon structures) dispersed in ionic liquids still generates controversy (Riazi et al., 2016), it has been recently demonstrated the possible enhancement of thermal energy

* Corresponding author.
E-mail address: mondragn@uji.es (R. Mondragón).

https://doi.org/10.1016/j.mechmat.2021.103886
Received 17 June 2020; Received in revised form 26 March 2021; Accepted 15 April 2021
Available online 24 April 2021
0167-6636/© 2021 The Authors. Published by Elsevier Ltd. This is an open access article under the CC BY license (http://creativecommons.org/licenses/by/4.0/).

storage of TES material with the addition of metallic nanoencapsulated Phase Change Materials (nePCMs) (Navarrete et al., 2017, 2019; Cingarapu et al., 2013, 2015) due to the contribution of the latent heat. These nanoencapsulated particles are composed of a phase change core wrapped in a surrounding shell made of another material with a melting temperature higher than that of the core. The role of the shell is to confine the core material when melting occurs. One of the main features of metallic nePCMs for TES applications is that they contribute considerably to increase the overall energetic performance of the nanofluid thanks to the latent heat absorbed/released during the phase change of their core. Moreover, they can be self-encapsulated with an oxide shell formed by natural passivation during the sintering process that can interact with the base fluid increasing the sensible heat in ionic liquids. In this context, optimising the design of the nePCMs is of key importance given that they play a direct influence on the performance of the nanofluid. One of the main problems encountered when nePCMs undergo thermal cycles is that their shell may fail mechanically, as it has been reported in (Navarrete et al., (2017)). The thermal stresses arising in the shells of the nePCMs could be one of the reasons for this failure, as investigated in (Forner-Escrig et al., (2020)).

Despite the fact that synthesis of nePCMs is performed experimentally with the valuable knowledge of the experimental community, the current work presents a numerical tool to analyse the behaviour of nePCMs from a quantitative perspective to get a better understanding of the physical phenomena involved in the failure of the nanoparticle shells. Furthermore, experimental measurements of the different material properties of a substance are not exempt from uncertainties, which are intrinsic to the nature of the measurement process. For this reason, it is important to numerically check the influence and consequences of these uncertainties on the measurements of the material properties by using a probabilistic technique that combines both Monte Carlo (MC) (Kroese et al., 2011) and Finite Element (FE) methods. In the same vein, considerable dispersion exists normally in the mean size of the synthesised nePCMs (Navarrete et al., 2017) and despite possessing a spherical morphology, they are not perfect spheres. Therefore, this lack of symmetry could have an impact on the mechanical failure of the shell of the nePCMs, which needs to be quantitatively assessed. Consequently, the study of all the aforementioned uncertainties on the nePCMs highlights the need of considering probabilistic analyses to evaluate the performance of these nanoparticles for TES applications in a wide range of temperature such as cold TES, comfort applications or high-temperature thermal management systems.

Some examples of probabilistic and numerical analyses are reported in the literature to analyse the failure of polymeric nanoparticle composites (Hamdia et al., 2017), and to optimise the nanoparticle wet milling process (Hou et al., 2007). However, neither their scope of analysis is the same as the one intended in the present work (nePCMs) nor the number of input parameters of their probabilistic analysis is large enough to analyse the influence of different physical parameters on their aim of study. Notice that the present work considers a set of 22 physical parameters (18 material and 4 geometrical parameters) to account for its influence on the failure of the nePCMs and, consequently, the analytical computation of the probability of failure may be complex. Then, the need for numerical methods arises.

MC simulation is a class of algorithms that use statistical sampling techniques to obtain a probabilistic approximation to the solution of a model: the samples previously generated are the inputs of the model and its evaluations provide the probabilistic outputs or responses of the model (Aderibigbe, 2014). The evaluation of the model may be performed by using analytical solutions or numerical methods such as the FE (Pérez–Aparicio et al., 2012; Palma et al., 2013, 2018), finite difference (Li and Rankin, 2010), finite volume (Bhoi and Sarkar, 2020), etc.

On this ground, the aim of the current work is to study two key magnitudes of nePCMs for TES applications: the maximum equivalent stress and the energy density capability and, to achieve this goal, reliability, uncertainty and sensitivity analyses are developed. In particular, two different pairs of nePCM materials are considered: tin encapsulated in tin oxide and aluminium encapsulated in aluminium oxide (alumina). For this purpose, a probabilistic tool is obtained by combining both MC and FE methods. The former considers up to 22 random variables and the input samples are generated by using the Latin Hypercube Sampling (LHS) technique (McKay et al., 1979), while the latter is a thermomechanical with phase-change FE code previously developed by the authors of the present work (Forner-Escrig et al., 2020). From the uncertainty analysis, distributions of maximum Rankine's equivalent stress –failure criterion for the shell– and of energy density are obtained. Furthermore, the sensitivity analysis permits to assess which of the 22 random variables exerts more influence on both the failure of the nePCM and on its energy density performance. With regard to the reliability analysis, both a deterministic and a probabilistic failure criterion are considered to verify its influence on the number of predicted failures when uncertainty in tensile strength exists. In conclusion, the results of these analyses may contribute to identify what are the physical parameters to be considered in advance to synthesise mechanically reliable nePCMs.

2. Outline of the problem

This section briefly reviews the model of the nePCM retained for the probabilistic analyses henceforth.

2.1. Description of the nanoparticle

The numerical model considers a single three-dimensional ellipsoidal nePCM, as that sketched in Fig. 1 a), where the geometry is defined by the three semi-axes a, b and c of the outer ellipsoid and the shell thickness e_{shell}. Notice that an ellipsoidal geometry for nePCMs is assumed in the present work for two reasons: i) to consider the influence of the geometrical uncertainty in the probabilistic analyses and ii) given that real nePCMs are not perfectly spherical. Fig. 1 b) depicts the mesh of an ellipsoidal nePCM and its appearance is quasi-spherical since the dispersion around the nominal values of the semi-axes is only of 5% (see Section 3.1 and Table 1).

Two different pairs of core@shell materials for nePCMs are considered: Sn@SnO_2 (tin encapsulated in tin oxide) and Al@Al_2O_3 (aluminium encapsulated in alumina). Their material properties are obtained from (Perry et al., 2008; Handbook Volume 2: Pr, 1990; Cverna, 2002; Stankus and Khairulin, 2006; Assael et al., 2017) for Sn, from (Landolt-Börnstein, (1998); Gaillac and Coudert, (2019); Gaillac et al., (2016); United States National In, (2901); Nam et al., (2017)) for SnO_2, from (Perry et al., (2008); andbook Volume 2: Pr, (1990); Cverna, (2002); The Engineering ToolBox., (2019)) for Al and from (Perry et al., (2008); Lynch, (1989); Shackelford et al., (2015); Accuratus Corporation and "A, (2019)) for Al_2O_3 and all of them are reported in Table 1. The material properties listed in Table 1 are mass density ρ, specific heat capacity at constant pressure c_p, thermal conductivity κ, Young's modulus E, Poisson's ratio ν, thermal expansion coefficient α, melting temperature T_m and latent heat L. Subscripts s and l denote solid and liquid state, respectively. For the geometry, an order of magnitude of the size of spherical Sn and Al nanoparticles may be obtained from (Navarrete et al., (2017)) and (Sarathi et al., 2007; Sahu and Hiremath, 2017; Navarrete et al., 2019), respectively.

Concerning the boundary and initial conditions, the nePCM is mechanically fixed at its centre and subjected to an initial temperature T_i. Then, an increasingly linear temperature is applied at the outer surface of the shell until a value of temperature T_0 (higher than the melting temperature of the core material) is reached. Concretely, $T_i = 323.15$ (K), $T_0 = 523.15$ (K) for Sn@SnO_2 and $T_0 = 973.15$ (K) for Al@Al_2O_3 nePCMs are considered.

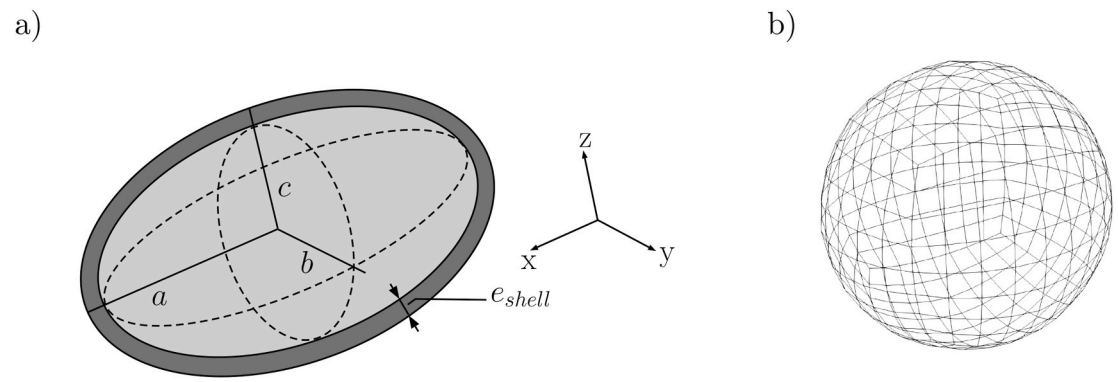

Fig. 1. a) Sketch of a generic ellipsoidal nanoencapsulated phase change material with the three semi-axes a, b and c of the outer ellipsoid and the shell thickness e_{shell}. b) Mesh of an ellipsoidal nanoencapsulated phase change material.

Table 1
Summary of material and geometrical properties of Sn@SnO_2 and Al@Al_2O_3 (core@shell) nanoencapsulated phase change materials (nePCMs). SRC is the abbreviation of standardised regression coefficients used in the sensitivity analysis and σ is the standard deviation for each of the properties with respect to their mean values.

	SRC	Property	Sn@**SnO_2** nePCMs	Al@**Al_2O_3** nePCMs	Units	σ(%)
Core	Θ_1	ρ_s	7280	2681	kg/m^3	5
	Θ_2	ρ_l	6800	2365	kg/m^3	5
	Θ_3	$c_{p,s}$	230	959.11	J/(kg K)	5
	Θ_4	$c_{p,l}$	257	1085.95	J/(kg K)	5
	Θ_5	κ_s	65	240	W/(m K)	5
	Θ_6	κ_l	31	93	W/(m K)	5
	Θ_7	E	43.3	70	GPa	5
	Θ_8	ν	0.33	0.33	–	5
	Θ_9	α_s	$2{\cdot}10^{-5}$	$2.1{\cdot}10^{-5}$	1/K	5
	Θ_{10}	T_m	498.65	933.15	K	5
	Θ_{11}	L	60.627	395.60	kJ/kg	5
Shell	Θ_{12}	ρ	7020	3970	kg/m^3	5
	Θ_{13}	c_p	348.95	919.38	J/(kg K)	5
	Θ_{14}	κ	40	10	W/(m K)	5
	Θ_{15}	E	222.72	370	GPa	5
	Θ_{16}	ν	0.284	0.24	–	5
	Θ_{17}	α	$4{\cdot}10^{-6}$	$8.2{\cdot}10^{-6}$	1/K	5
	Θ_{18}	T_m	1900	2273.15	K	5
Geometry	Θ_{19}	a	40	40	nm	5
	Θ_{20}	b	40	40	nm	5
	Θ_{21}	c	40	40	nm	5
	Θ_{22}	e_{shell}	7	7	nm	5

2.2. Description of the finite element model

The evaluation of the nanoparticle model is performed by a three-dimensional FE code developed by the authors. In particular, a thermodynamically consistent FE formulation was developed in (Forner-Escrig et al., (2020)) by considering thermomechanical coupling and three phase change approaches: enthalpy, heat source and heat capacity. This formulation was implemented in the research code FEAP (Taylor, 2013), which belongs to the University of California at Berkeley (USA).

Numerically, the FE formulation is monolithic and eight-noded with four degrees of freedom (dof) per node:

$$\text{dof} = \left\{ \underline{u}, T \right\}, \tag{1}$$

where the first term in brackets represents the three components of the displacement field $\underline{u} = \{u, v, w\}$ and the last term is the temperature. These dofs are discretised by using standard shape functions of Lagrangian type. For the sake of brevity, only the tangent matrix is reported in the present work:

$$\begin{bmatrix} \mathscr{K}^{\underline{u}\,\underline{u}}_{ab} + c_3\, \mathscr{M}^{\underline{u}\,\underline{u}}_{ab} & \mathscr{K}^{\underline{u}\,T}_{ab} \\ 0 & \mathscr{K}^{T\,T}_{ab} \end{bmatrix} \tag{2}$$

where $\mathscr{K}$ and $\mathscr{M}$ denote stiffness and mass matrices, respectively. Subscripts a and b refer to discretisation nodes while superscripts denote the dofs. As observed, only a one-way coupling is considered with the term $\mathscr{K}^{\underline{u}\,T}_{ab}$, which is due to the thermomechanical volumetric expansion. With regard to the time integration scheme, the scalar coefficient c_3 in (2) is associated to the Newmark−β algorithm. Finally, the enthalpy approach is used in the current work.

3. Probabilisitic analysis

The present work uses a probabilistic numerical tool that combines the thermomechanical FE method with the MC technique. As shown in Fig. 2, the working principle of this tool consists of:

1. Identifying the random parameters and their distribution functions.
2. Generating a random sample of size N.
3. Performing N evaluations of the model through the FE code.
4. Analyse the N outputs of the FE code: Uncertainty Analysis (UA), Sensitivity Analysis (SA), Probability of Failure (POF) and Energy Density (E_d) distribution.

3.1. Distribution functions and sample generation

Firstly, the j random variables ξ_j –commonly called parameters– of the model must be identified and quantified in accordance with experimental observations. In the present work, all the material and geometrical properties ($j = 1, \ldots, 22$) of the nePCM are considered as random variables; their nominal values and standard deviation (uncertainty) of the random variables are shown in Table 1.

Secondly, neither the distribution function of the measurements of these variables nor most of uncertainties in the measurement process are available in the literature. However, the experimental values of physical properties are normally obtained as the average of the different measurements and, therefore, according to the central limit theorem, these values can be assumed to be normally distributed even when the original samples themselves do not obey a normal distribution.

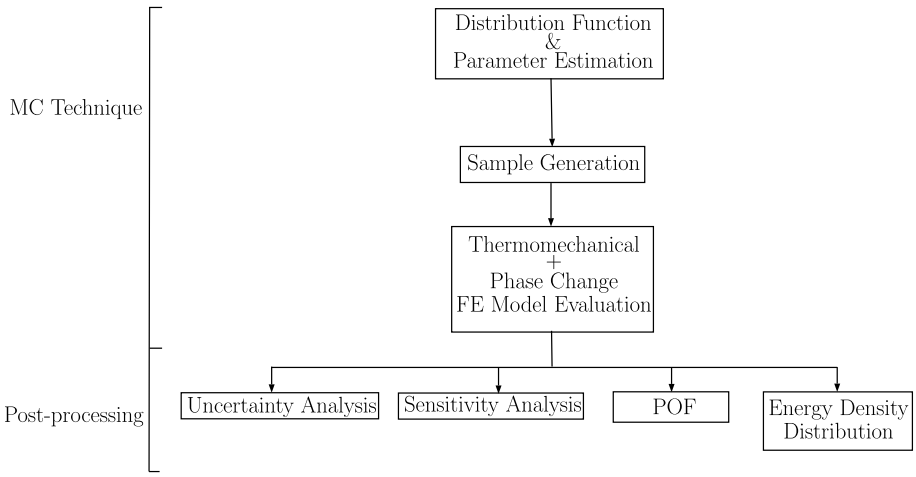

Fig. 2. Flowchart of the probabilistic numerical tool.

According to the orders of magnitude of dispersion in measurements reported in (Perry et al., (2008)), a standard deviation σ of 5% around the nominal value (mean) of each material parameter is considered as a first and good estimation. With regard to geometrical parameters and in agreement with the experimental characterisations available in (Navarrete et al., 2017, 2019), the size of nePCMs is assumed to be log-normally distributed. In particular, the mean size and standard deviation of the log-normal distribution for the generation of the nominal value of the outer ellipsoid size are 40 [nm] and 40% around the mean value, respectively. Since experimentally it is observed that nanoparticles are not perfect spheres but quasi-spherical, an ellipsoidal geometry is defined with a standard deviation of 5% around the previously generated log-normal values of the nanoparticle size. Notice that the shell thickness is uniform around the core of a single nePCM but its nominal value can vary for the different nePCMs within a 5% of uncertainty by following a normal distribution.

Finally, the LHS technique (McKay et al., 1979) is used to generate the random samples. LHS is a statistical technique to generate random numbers which consists of dividing the cumulative density function of each random variable into N equal partitions and choosing a random data point in each partition of each random variable. Then, the samples of each random variable are combined in order to create the set of random input vectors of the model. This technique is used in the present work for two reasons: i) it reduces the computational time (Olsson et al., 2003) with respect to the time required for standard random sampling, and ii) the random sample generated is more representative of the variability of the random variables than standard random generations.

3.2. Uncertainty and sensitivity analyses

Consider a generic model M represented by the mathematical expression:

$$\phi_i = M(\xi_j), \tag{3}$$

where ϕ_i represents the i outputs and ξ_j the j inputs.

On the one hand, the main goal of the UA is to determine the uncertainty in the model output when the uncertainties in the input are known. Concretely, UA allows to calculate the probability distribution of the output and their scalar parameters: mean and standard deviation.

On the other hand, the objective of the SA is to determine the relationship among the uncertainties in input and output variables, namely, SA permits to identify which input variables exert more influence on the response of the model. Although there are different techniques to develop a SA (Saltelli et al., 2008), multiple linear regression is adopted in the present work. According to (Montgomery and Runger, (2003); Palma et al., 2009), in multiple linear regression, each output ϕ_i may be approximated by:

$$\phi_i \approx \theta_0 + \sum_{j=1}^{N_\xi} \theta_j \xi_j + \Psi, \tag{4}$$

where N_ξ represents the number of random variables (or inputs) of the model, θ_j are the regression coefficients that relate each input ξ_j with each output ϕ_i, θ_0 is the intercept term of the linear regression and Ψ represents a random error term.

Regression coefficients θ_0 and θ_j are determined by least-square computation from (4) and, despite the fact that they provide information on the relationship between the inputs and outputs of the model, according to (Saltelli et al., (2008)), regression coefficients are not an appropriate sensitivity measure. Instead, another sensitivity measure known as Standardised Regression Coefficients (SRC) is preferred and they are defined as:

$$\Theta_j = \theta_j \frac{\sigma_{\xi_j}}{\sigma_{\phi_i}}, \tag{5}$$

where σ_{ξ_j} and σ_{ϕ_i} denote the standard deviations of input and output, respectively. SRC are recommended measures for SA since they account not only for raw regression coefficients but also for standard deviations of both inputs and outputs and then provide a normalised measure of the importance of the input parameters on the response of the model (Saltelli et al., 2008). Thus, SRC are the sensitivity measures considered through the present work.

3.3. Probability of failure

The POF, which is a statistical indicator of the frequency of occurrence of a considered failure event, is mathematically defined as (Melchers and Beck, 2018):

$$\mathrm{POF} = P\left[G(\xi_j) \le 0\right] = \int_{G(\xi_j)\le 0} f_{\xi_j}(\Xi)\mathrm{d}\Xi, \tag{6}$$

where ξ_j, $G(\xi_j)$ and $f_{\xi_j}(\Xi)$ represent the vector of input random variables, a limit state function and the joint probability density function of the input random variables, respectively. Therefore, $G(\xi_j) \le 0$ refers to the region where the limit state violation occurs, i.e. the failure region. In general, equation (6) cannot be evaluated analytically, except for some special cases, but the POF can still be determined numerically. One of the existing techniques to compute this POF numerically is MC techniques and according to (Melchers and Beck, (2018)), for these

techniques, the POF can be evaluated as:

$$\text{POF} \approx \frac{n\left[G\left(\widehat{\Xi}_j \leq 0\right)\right]}{N}, \tag{7}$$

where $n[G(\widehat{\Xi}_j \leq 0)]$ is the number of trials n for which the limit state function is not satisfied, i.e. $G(\widehat{\Xi}_j \leq 0)$. In (7), $\widehat{\Xi}_j$ is used to represent a sample value of each random variable.

As well known, the number of total trials N determines the desired accuracy of the POF, which may be measured by the Coefficient of Variation (CV) of the POF (Smarslok et al., 2010):

$$\text{CV}_{POF} = \sqrt{\frac{1-\text{POF}}{N \cdot \text{POF}}}. \tag{8}$$

Then, the larger N, the most accurate POF is but, in contrast, choosing large values of N increases considerably the computational cost and, therefore, an agreement between accuracy and computation time must be reached. The value of N used in the present work and the time needed to run these simulations is detailed in Section 4.1.

4. Results

This section summarises the results obtained from the probabilistic tool for both Sn@SnO_2 and Al@Al_2O_3 nePCMs.

4.1. Uncertainty analysis

Two UA for two nePCMs –Sn@SnO_2 and Al@Al_2O_3– are conducted in order to obtain two outputs of the model (3):

i) The maximum Rankine's equivalent stress σ_R distribution on the nePCM shell: $\phi_1 = \sigma_R$, see Fig. 3.
ii) The energy density E_d of the nePCMs: $\phi_2 = E_d$, see Fig. 4.

Notice that these outputs are selected among others since they are key magnitudes in the design and optimisation of nePCMs for TES applications.

With regard to the equivalent stress distribution and in agreement with (Forner-Escrig et al., 2020), Rankine's criterion is used to predict the mechanical failure of the nePCM, which usually occurs at the shell.

Fig. 3 shows the histogram and the statistical scalar values (mean μ and standard deviation σ) after running the UA. As observed, these scalar values are $\mu = 407.25$ [MPa], $\sigma = 71.80$ [MPa] for Sn@SnO_2 and $\mu = 1836.80$ [MPa], $\sigma = 250.62$ [MPa] for Al@Al_2O_3. Despite the fact that deterministic values do not exist in literature to validate these results, their tendency appear to be logical since larger values of stress are more likely to occur in Al@Al_2O_3. Notice that the melting temperature of the Al core is considerably higher than that of Sn; consequently, larger thermal stresses are expected to arise in the Al@Al_2O_3 nePCMs to reach the liquid state of the core.

In order to measure the accuracy of the predicted σ_R, a bilateral Confidence Interval (CI) around the mean μ is defined as:

$$\text{CI}_{1-\alpha} = \mu \pm SE \cdot t_{\alpha,N-1}, \tag{9}$$

where α represents the risk –also called significance level– of the CI and t_{N-1} is the Student's t-distribution with $N-1$ degrees of freedom. The Standard Error (SE) of μ is defined as:

$$\text{SE} = \frac{\sigma}{\sqrt{N}}. \tag{10}$$

The CI for the equivalent stress at a significance level of $\alpha = 5\%$ is {393.03, 421.47} [MPa] for Sn@SnO_2 nePCMs and {1787.17, 1886.42} [MPa] for Al@Al_2O_3 nePCMs.

Regarding energy density E_d, which is a relevant magnitude for energy storage purposes, the metric used in the present work for its quantification is defined as:

$$E_d = \rho_l L \frac{V_{core}}{V_{total}}, \tag{11}$$

where V_{core} and V_{total} denote the core and total volume of the nePCM, respectively.

Fig. 4 represents the histogram and scalar values of E_d for Sn@SnO_2

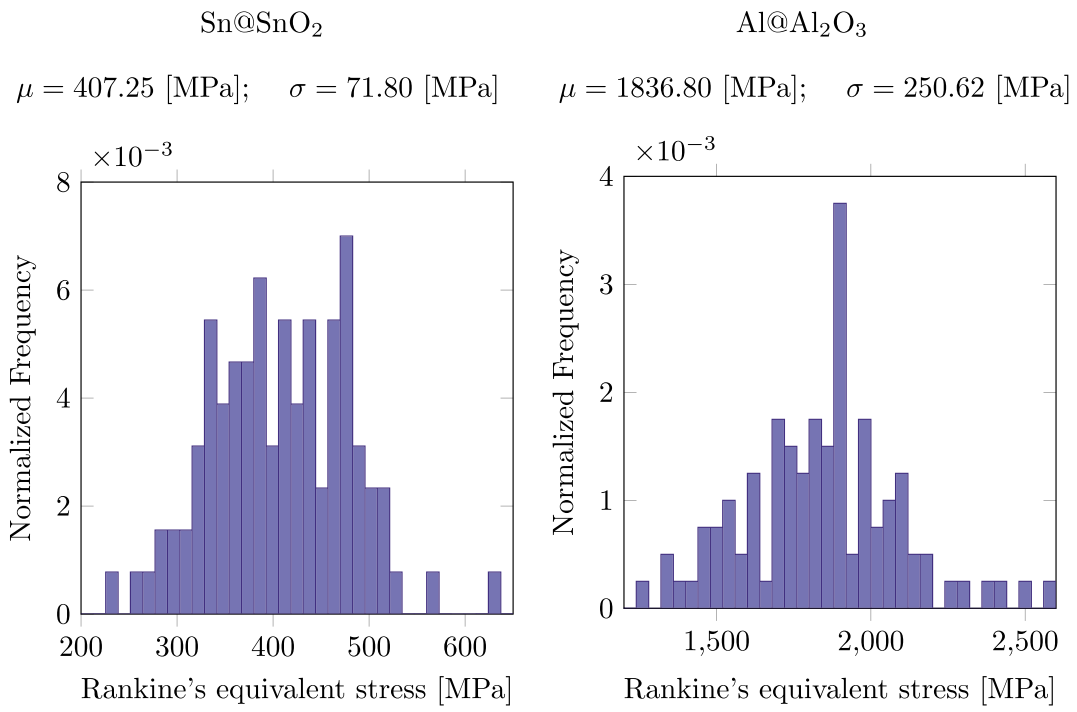

Fig. 3. Histogram of Rankine's equivalent stress for Sn@SnO_2 nePCMs (left) and Al@Al_2O_3 nePCMs (right) with their respective mean value μ and standard deviation σ.

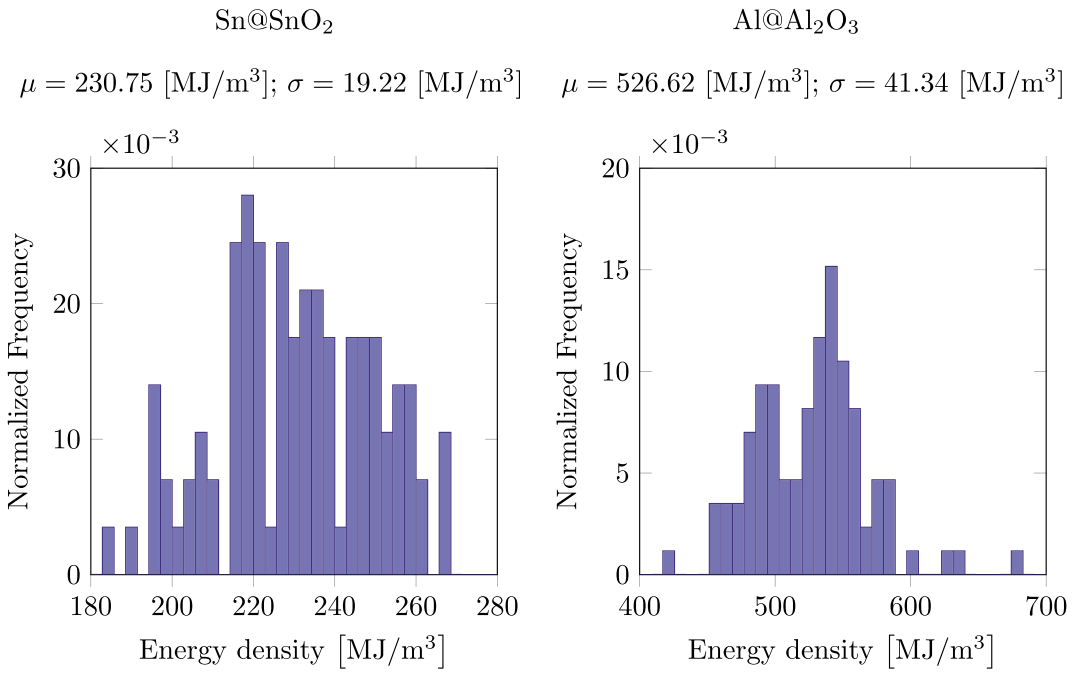

Fig. 4. Histogram of energy density for $Sn@SnO_2$ nePCMs (left) and $Al@Al_2O_3$ nePCMs (right) with their respective mean value μ and standard deviation σ.

and $Al@Al_2O_3$ nePCMs. From (9), the E_d for $Sn@SnO_2$ nePCMs is found to lie in the confidence interval $CI_{0.95} = \{226.94, 234.56\}$ [MJ/m^3] with $\mu = 230.75$ [MJ/m^3], while for $Al@Al_2O_3$, $CI_{0.95} = \{518.43, 534.81\}$ [MJ/m^3] with $\mu = 526.62$ [MJ/m^3]. From these results, it can be concluded that the energetic performance of Al nePCMs is better than that of Sn ones.

Two numerical verifications are performed: statistical and convergence tests. On the one hand, the Jarque-Bera test (Jarque and Bera, 1987) is used to determine if the null hypothesis –a data sample comes from a normal distribution at a certain significance level– is accepted. The Jarque-Bera test is applied to both σ_R and E_d and it is found that both distributions and both pairs of core@shell materials are normally distributed at a significance level of 1%. Notice that the linearity assumption is not obvious since the present probabilistic analysis combines normal and log-normal distributions.

On the other hand, the sample size N to guarantee a proper convergence of the MC is performed by a trial and error numerical test since obtaining a general analytic expression to pre-calculate N for convergence of MC simulations is difficult or even impossible for complex models. The numerical test consists of representing the average evolution of μ and σ versus the number of iterations, as observed in Fig. 5. From this figure, it can be concluded that the numerical simulation converges for $N = 100$ iterations and that is the value used through the present work. For this sample size, the computational time

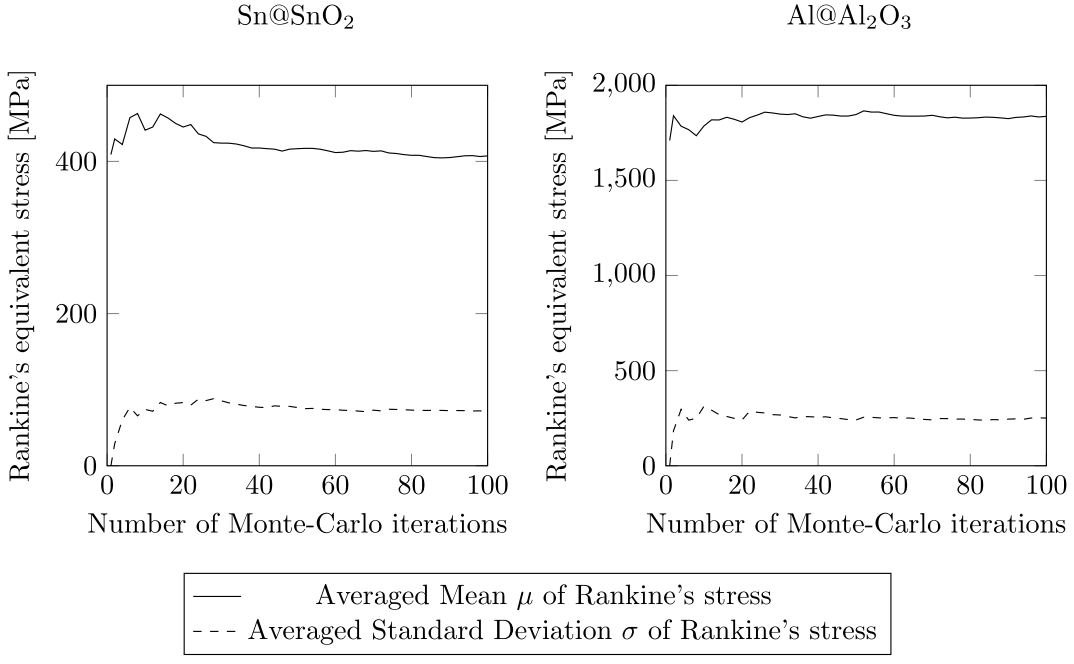

Fig. 5. Convergence of Monte Carlo simulation.

is approximately 14 h for a PC with a processor Intel® Core™i7-950 and 16 GB of RAM.

4.2. Sensitivity analysis

A multiple linear regression is performed to develop the SA in order to calculate the influence of the random variables ξ_j on the σ_R for both $Sn@SnO_2$ and $Al@Al_2O_3$ nePCMs. This influence is shown in Fig. 6 by a bar diagram for the different absolute values of the SRC, see notation in Table 1.

Firstly, the SRC values obtained for each nePCM are not the same given that the material properties are different. However, the same tendency may be observed in both of bar diagrams.

Secondly, the most relevant random values appear to be Θ_8, Θ_9 and Θ_{10}, which represent the Poisson's ratio of the core, the thermal expansion coefficient of the core and its melting temperature, respectively. These results seem to be in good agreement with physical intuition: the latter plays a direct role in the maximum value of stress reached until the melting of the core, and the thermal expansion coefficient and the Poisson's ratio are parameters that mechanically govern the volumetric changes in nePCMs.

Thirdly, the next set of parameters having more influence on the failure are the geometrical ones: Θ_{19}, Θ_{20}, Θ_{21} and Θ_{22}. The three first parameters stand for the semi-axes of the ellipsoidal nePCM and the last one represents the shell thickness. The difference in values between $Sn@SnO_2$ and $Al@Al_2O_3$ nePCMs for the SRC of the three semi-axes in Fig. 6 is not very significant and could be influenced by randomness in the generation of the random samples.

Finally and since multiple linear regression is applied for this sensitivity analysis, the validity of the hypothesis of linearity must hold true for the results to be acceptable. In order to verify the validity of the SA, the coefficients of determination of the linear regression are $R^2_{Sn} = 0.93$ and $R^2_{Al} = 0.92$ for the $Sn@SnO_2$ and $Al@Al_2O_3$, respectively. According to (Pan et al., (2011); Saltelli et al., (2006)), as long as the coefficient of determination verifies $R^2 \geq 0.7$, the linearity hypothesis is satisfied and thus, the present SA is valid as well.

Notice that the random variables ξ_j exerting a major influence on E_d can be directly determined from its definition in Equation (11) without need of performing a SA. Therefore, the latent heat of the core, the mass density of the liquid core and the geometrical parameters are the variables that have a more relevant impact on E_d.

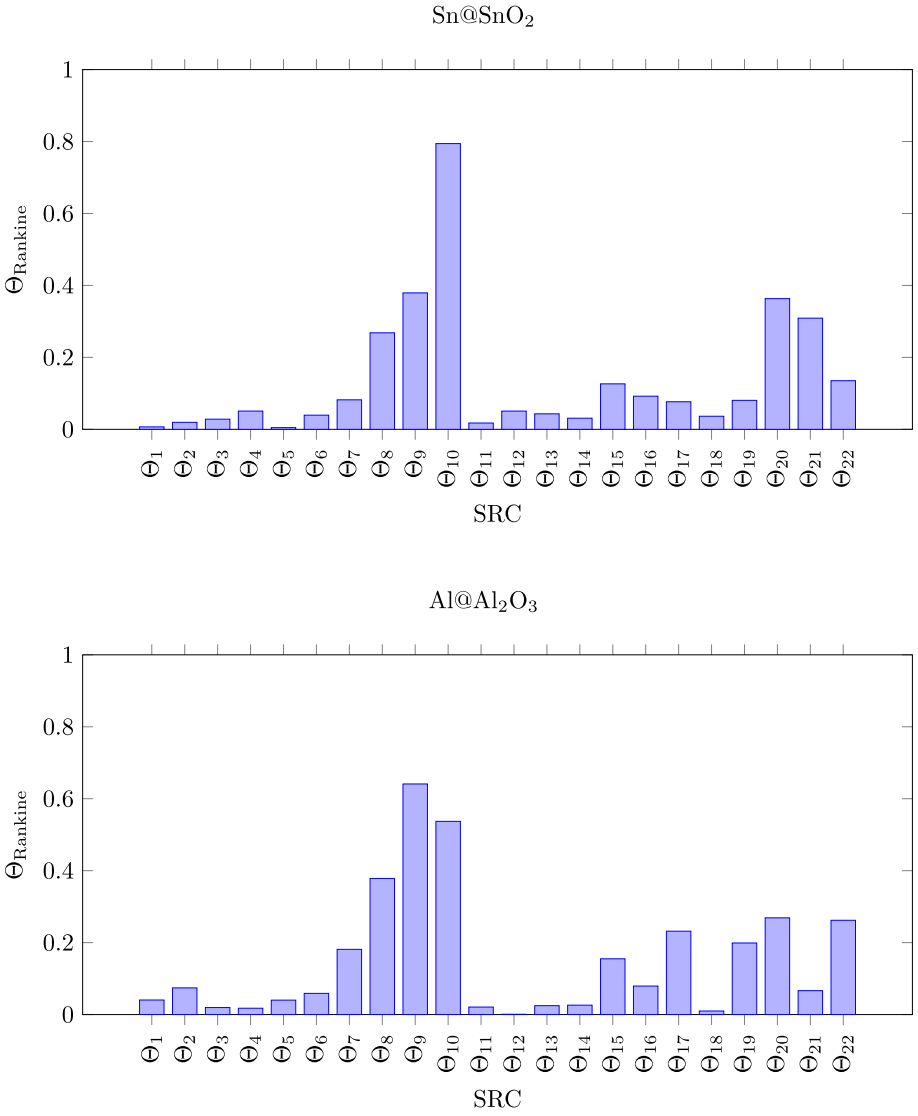

Fig. 6. Standardised Regression Coefficients (SRC) in absolute value for $Sn@SnO_2$ (top) and $Al@Al_2O_3$ (bottom) nanoencapsulated phase change materials. Notation in Table 1.

4.3. Probability of failure of nePCMs

In this section, the POF of $Sn@SnO_2$ and $Al@Al_2O_3$ nePCMs is calculated by using both deterministic and probabilistic failure criteria:

- The deterministic criterion consists of using a tensile strength σ_t value from literature and studying its position with respect to the σ_R distribution obtained from the probabilistic simulations.
- The probabilistic criterion is grounded on the uncertainty in the measure of σ_t, resulting in a tensile strength distribution. According to (8), by considering a probabilistic criterion to compute the POF, the accuracy of the MC simulation is increased by a factor $\sqrt{N}$ –a factor of 10 in the present simulations. Notice that this motivates the need for considering a probabilistic failure criterion.

Concerning $Sn@SnO_2$ nePCMs, $\sigma_t = 803$ [MPa] is assumed for SnO_2 (Nam et al., 2017) for the deterministic case. According to (Nam et al., (2017)), the tensile strength of SnO_2 may suffer from fluctuations due to its porosity, which is a hard to control parameter when synthesising nePCMs. Consequently, σ_t is assumed to be normally distributed with a 20% of dispersion around $\sigma_t = 803$ [MPa] for the probabilistic criterion. This percentage of 20% is considered as a first approximation from the measurement dispersion existing in the characterisation of tensile strength of metals at the macroscale and by assuming that a considerable error may be induced by the different behaviour of this mechanical property between the macro and the nanoscale.

Fig. 7 shows the σ_R distribution for both deterministic (top) and probabilistic (bottom) criteria. For the deterministic criterion, σ_R falls below the deterministic σ_t and, consequently, the POF of is 0%: any nePCM is expected to fail.

On the contrary and for the probabilistic criterion, it can be observed that there is an overlap between the Gaussian curve of the σ_R distribution and that of the probabilistic σ_t. This overlapping region represents the area in the graph where the nePCMs are likely to fail mechanically. In this case, the POF becomes 1.87% and this means that it is advisable to account for these type of criterion, especially when dispersion in tensile strength exists.

It is important to highlight that the present results are in accordance with the experimental observations reported in (Navarrete et al., (2017)), given that only small samples of $Sn@SnO_2$ nePCMs were verified to fail mechanically due to thermal stresses.

With regard to $Al@Al_2O_3$ nePCMs, to the best of the author's knowledge, experimental data on the mechanical failure of $Al@Al_2O_3$ nePCMs is not available in the literature. In the present work, $\sigma_t = 275.9$ [MPa] (Shackelford et al., 2015) with a Gaussian dispersion of 20% is considered, as in the previous case.

Fig. 8 shows the distribution of the σ_R with the deterministic (top) and the probabilistic (bottom) failure criteria. For this material, the POF predicted for both deterministic and probabilistic criteria is 100% since the distribution of σ_R obtained is far above the tensile strength.

In conclusion, despite the fact that $Al@Al_2O_3$ nePCMs possess larger energy density storage capabilities than $Sn@SnO_2$ nePCMs, the first ones are likely to fail mechanically when they undergo heating cycles.

5. Conclusions

This article has presented a numerical tool, which combines Monte Carlo techniques and a thermomechanical finite element with phase change, in order to conduct probabilistic analyses –uncertainty, sensitivity and reliability– in nanoencapsulated phase change materials (nePCMs). In particular, experimental uncertainties are taken into account to obtain the mechanical probability of failure and this mechanical failure is one of the problems experimentally encountered when the nePCMs undergo thermal processes. In addition, the sensitivity analysis has allowed to quantify the parameters that exert the most significant

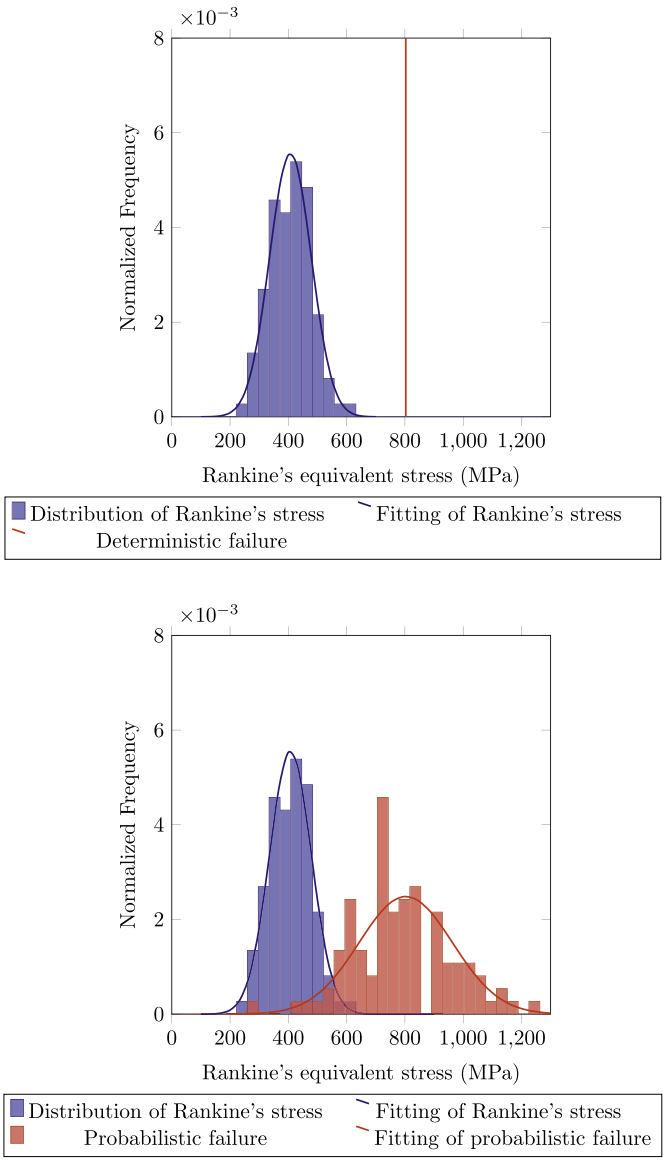

Fig. 7. Deterministic (top) and probabilistic (bottom) failure criteria compared against the maximum Rankine's equivalent stress obtained from Monte Carlo simulation for $Sn@SnO_2$ nanoencapsulated phase change materials.

influence on the mechanical failure of nePCMs. Consequently, these relevant parameters should be closely controlled in the synthesis of nanoparticles.

Specifically, the present work has considered 22 random parameters −18 material properties and 4 geometrical parameters– and has studied the evolution of two variables – Rankine's equivalent stress and energy density– for two nePCMs: $Sn@SnO_2$ and $Al@Al_2O_3$. Firstly and from the sensitivity analysis, it has been concluded that the melting temperature, thermal expansion coefficient and Poisson's ratio exert the more relevant influence on the mechanical failure of the nanoparticle shell. In turn, the most influential parameters on the energy density capability of nePCMs are the latent heat of the core, the mass density of the liquid core and the geometrical parameters of the nePCM. Secondly, it has been concluded that the probabilistic failure is 1.87% and 100% for $Sn@SnO_2$ and $Al@Al_2O_3$ nePCMs, respectively. The results of the former are verified to be in good agreement with experimental observations while, to the author's knowledge, no data is available for the latter ones.

To sum up, the numerical probabilistic tool allows to estimate the probability of failure of the nePCMs and to determine the parameters

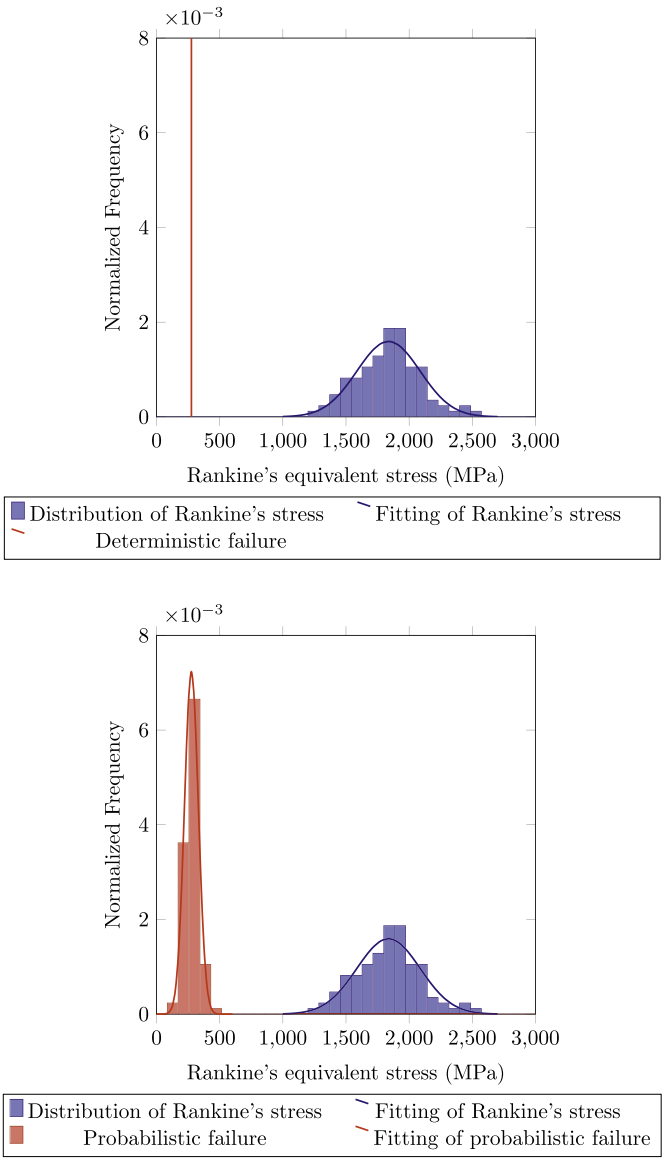

Fig. 8. Deterministic (top) and probabilistic (bottom) failure criteria compared against the maximum Rankine's equivalent stress obtained from Monte Carlo simulations for Al@Al_2O_3 nanoencapsulated phase change materials.

having a bigger influence on the failure and energy storage of nePCMs for their use in TES systems. The scope of the present numerical tool can be expanded to predict the mechanical failure of any micro and nano-encapsulated PCMs made of different pairs of core@shell materials as long as their material properties and measurement dispersion are known.

Finally, the present numerical probabilistic tool could be used to complement experimental research and to reduce the number of experiments to be conducted to optimise the selection of a pair of core and shell nePCMs by maximising the energy density and by minimising the probability of the failure of the shell.

Author statement

Joser Forner-Escrig: Conceptualization, Methodology, Data curation, Formal analysis, Writing – original draft, Writing – review & editing. Rosa Mondragón: Conceptualization, Data curation, Writing – review & editing, Supervision. Leonor Hernández: Data curation, Writing – review & editing. Roberto Palma: Conceptualization, Methodology, Data curation, Formal analysis, Writing – original draft, Writing – review & editing, Supervision

Declaration of competing interest

The authors declare that they have no known competing financial interests or personal relationships that could have appeared to influence the work reported in this paper.

Acknowledgements

This research was partially funded by *Ministerio de Economía y Competitividad (MINECO)* of Spain through the project ENE2016-77694-R. Josep Forner-Escrig thanks *Ministerio de Economía, Industria y Competitividad* of Spain and Fondo Social Europeo for a pre-doctoral fellowship through Grant Ref. BES-2017-080217 (FPI program). This work has been developed by participants of the COST Action CA15119 Overcoming Barriers to Nanofluids Market Uptake (NANOUPTAKE).

References

Accuratus Corporation. Aluminum oxide, Al_2O_3 ceramic properties. https://accuratus.com/alumox.html. (Accessed 18 August 2019).
Aderibigbe, A., 2014. A Term Paper on Monte Carlo Analysis/Simulation. *Department of Electrical and Electronic Engineering.* Faculty of Technology. University of Ibadan.
Akhmetov, B., Georgiev, A.G., Kaltayev, A., Dzhomartov, A.A., Popov, R., Tungatarova, M.S., 2016. Thermal energy storage systems - review. Bulgarian Chemical Communications. Special Issue E 48, 31–40.
ASM Handbook Volume 2: Properties and Selection: Nonferrous Alloys and Special-Purpose Materials, 1990. ASM International, Materials Park.
Assael, M.J., Chatzimichailidis, A., Antoniadis, K.D., Wakeham, W.A., Huber, M.L., Fukuyama, H., 2017. Reference correlations for the thermal conductivity of liquid copper, gallium, indium, iron, lead, nickel and tin. High. Temp. - High. Press. 46, 391–416.
Bhoi, S., Sarkar, D., 2020. Hybrid finite volume and Monte Carlo method for solving multi-dimensional population balance equations in crystallization processes. Chem. Eng. Sci. 217, 115511.
Choi, S., Eastman, J., 1995. Enhancing thermal conductivity of fluids with nanoparticles. In: Proceedings of the ASME International Mechanical Engineering Congress and Exposition, San Francisco, CA, USA.
Cingarapu, S., Singh, D., Timofeeva, E.V., Moravek, M.R., 2013. Nanofluids with encapsulated tin nanoparticles for advanced heat transfer and thermal energy storage. Int. J. Energy Res. 38, 51–59.
Cingarapu, S., Singh, D., Timofeeva, E.V., Moravek, M.R., 2015. Use of encapsulated zinc particles in a eutectic chloride salt to enhance thermal energy storage capacity for concentrated solar power. Renew. Energy 80, 508–516.
Cverna, F., 2002. ASM Ready Reference: Thermal Properties of Metals. ASM International, Materials Park.
Forner-Escrig, J., Palma, R., Mondragón, R., 2020. Finite element formulation to study thermal stresses in nanoencapsulated phase change materials for energy storage. J. Therm. Stresses 43 (5), 543–562.
Gaillac, R., Coudert, F.-X.. ELATE elastic tensor analysis. http://progs.coudert.name/elate/mp?query=mp-856. (Accessed 21 October 2019).
Gaillac, R., Pullumbi, P., Coudert, F.-X., 2016. Elate: an open-source online application for analysis and visualization of elastic tensors. J. Phys. Condens. Matter 28 (27), 275201.
Gil, A., Medrano, M., Martorell, I., Lázaro, A., Dolado, P., Zalba, B., Cabeza, L.F., 2010. "State of the art on high temperature thermal energy storage for power generation. part 1—concepts, materials and modellization. Renew. Sustain. Energy Rev. 14 (1), 31–55.
Hamdia, K.M., Silani, M., Zhuang, X., He, P., Rabczuk, T., 2017. Stochastic analysis of the fracture toughness of polymeric nanoparticle composites using polynomial chaos expansions. Int. J. Fract. 206 (2), 215–227.
Hou, T.-H., Su, C.-H., Liu, W.-L., 2007. Parameters optimization of a nano-particle wet milling process using the Taguchi method, response surface method and genetic algorithm. Powder Technol. 173 (3), 153–162.
International Energy Agency. (IEA), 2011. Solar Energy Perspectives. International Energy Agency, Paris.
International Energy Agency (IEA). World energy outlook. https://www.iea.org/weo/. (Accessed 11 July 2019).
Jarque, C.M., Bera, A.K., 1987. A test for normality of observations and regression residuals. Int. Stat. Rev./Rev. Int. Stat. 55 (2), 163–172.
Kroese, D.P., Taimre, T., Botev, Z.I., 2011. Handbook of Monte Carlo Methods. John Wiley & Sons, Inc., New York.
Landolt-Börnstein, 1998. Semiconductors. Non-tetrahedrally Bonded Elements and Binary Compounds I, 41C. Springer-Verlag Berlin Heidelberg, New York.
Li, X., Rankin, S.E., 2010. Multiscale dynamic Monte Carlo/continuum model of drying and nonideal polycondensation in sol-gel silica films. American Institue of Chemical Engineers Journal 56 (11), 2946–2956.
Lynch, C.T. (Ed.), 1989. Practical Handbook of Materials Science. CRC Press, Boca Raton.

McKay, M.D., Beckman, R.J., Conover, W.J., 1979. A comparison of three methods for selecting values of input variables in the analysis of output from a computer code. Technometrics 21 (2), 239–245.
Melchers, R.E., Beck, A.T., 2018. Structural Reliability Analysis and Prediction, third ed. John Wiley & Sons, Ltd., New York.
Mondragón, R., Navarrete, N., Gimeno-Furió, A., Hernández, L., Cabedo, L., Juliá, J.E., 2017. "New high-temperature heat transfer and thermal storage molten salt–based nanofluids: preparation, stabilization, and characterization. In: Minea, A.A. (Ed.), Advances In New Heat Transfer Fluids: from Numerical To Experimental Techniques, ch. 11. CRC Press, Boca Raton.
Montgomery, D.C., Runger, G.C., 2003. Applied Statistics and Probability for Engineers, third ed. John Wiley & Sons, Inc., New York.
Nam, K., Wolfenstine, J., Choi, H., Garcia-Mendez, R., Sakamoto, J., Choe, H., 2017. Study on the mechanical properties of porous tin oxide. Ceram. Int. 43, 10913–10918.
Navarrete, N., Gimeno-Furió, A., Mondragón, R., Hernández, L., Cabedo, L., Cordoncillo, E., Juliá, J.E., 2017. Nanofluid based on self-nanoencapsulated metal/metal alloys phase change materials with tuneable crystallisation temperature. Sci. Rep. 7.
Navarrete, N., Mondragón, R., Wen, D., Navarro, M.E., Ding, Y., Juliá, J.E., 2019. "Thermal energy storage of molten salt –based nanofluid containing nano-encapsulated metal alloy phase change materials. Energy 167, 912–920.
Olsson, A., Sandberg, G., Dahlblom, O., 2003. On Latin hypercube sampling for structural reliability analysis. Struct. Saf. 25 (1), 47–68.
Palma, R., Rus, G., Gallego, R., 2009. Probabilistic inverse problem and system uncertainties for damage detection in piezoelectrics. Mech. Mater. 41 (9), 1000–1016.
Palma, R., Pérez-Aparicio, J., Bravo, R., 2013. Study of hysteretic thermoelectric behavior in photovoltaic materials using the finite element method, extended thermodynamics and inverse problems. Energy Convers. Manag. 65, 557–563. Global Conference on Renewable energy and Energy Efficiency for Desert Regions 2011 'GCREEDER' 2011.
Palma, R., Torrent, J., Pérez-Aparicio, J.L., Ripoll, L., 2018. Reliability-based dynamical design of a singular structure for high energy physics experiments. Archives of Civil and Mechanical Engineering 18 (1), 256–266.
Pan, F., Zhu, J., Ye, M., Pachepsky, Y.A., Wu, Y.-S., 2011. Sensitivity analysis of unsaturated flow and contaminant transport with correlated parameters. J. Hydrol. 397 (3), 238–249.
Pérez–Aparicio, J., Palma, R., Taylor, R., 2012. Finite element analysis and material sensitivity of peltier thermoelectric cells coolers. Int. J. Heat Mass Tran. 55 (4), 1363–1374.
Perry, R.H., Green, D.W., Maloney, J.O., 2008. Perry's Chemical Engineers' Handbook. McGraw-Hill, New York.
Riazi, H., Murphy, T., Webber, G.B., Atkin, R., Tehrani, S.S.M., Taylor, R.A., 2016. Specific heat control of nanofluids: a critical review. Int. J. Therm. Sci. 107, 25–38.
Sahu, R.K., Hiremath, S.S., 2017. Synthesis of aluminium nanoparticles in A water/polyethylene glycol mixed solvent using μ-EDM. IOP Conf. Ser. Mater. Sci. Eng. 225, 012257.
Saltelli, A., Ratto, M., Tarantola, S., Campolongo, F., 2006. Sensitivity analysis practices: strategies for model-based inference. Reliab. Eng. Syst. Saf. 91 (10), 1109–1125. The Fourth International Conference on Sensitivity Analysis of Model Output (SAMO 2004).
Saltelli, A., Ratto, M., Andres, T., Campolongo, F., Cariboni, J., Gatelli, D., Saisana, M., Tarantola, S., 2008. Global Sensitivity Analysis. The Primer. John Wiley & Sons, Ltd., New York.
Sarathi, R., Sindhu, T., Chakravarthy, S., 2007. Generation of nano aluminium powder through wire explosion process and its characterization. Mater. Char. 58 (2), 148–155.
Shackelford, J.F., Han, Y.-H., Kim, S., Kwon, S.-H., 2015. CRC Materials Science and Engineering Handbook, fourth ed. CRC Press, Boca Raton.
Smarslok, B.P., Haftka, R.T., Carraro, L., Ginsbourger, D., 2010. Improving accuracy of failure probability estimates with separable Monte Carlo. Int. J. Reliab. Saf. 4 (4), 393–414.
Stankus, S.V., Khairulin, R.A., 2006. "The density of alloys of tin—lead system in the solid and liquid states. High Temp. 44, 389–395.
Taylor, R., 2013. FEAP A Finite Element Analysis Program: User Manual. University of California, Berkeley. http://www.ce.berkeley.edu/feap. (Accessed 21 October 2019).
The Engineering ToolBox. https://www.engineeringtoolbox.com. (Accessed 18 August 2019).
United States National Institutes of Health (NIH). PubChem open chemistry database. https://pubchem.ncbi.nlm.nih.gov/compound/29011. (Accessed 21 October 2019).
Xu, B., Li, P., Chan, C., 2015. Application of phase change materials for thermal energy storage in concentrated solar thermal power plants: a review to recent developments. Appl. Energy 160, 286–307.